Computational Electromagnetics for Efficient Control Design of Massive MIMO and Beyond

Lu Ou
College of Computer Science and Electronic Engineering
Hunan University
Changsha, Hunan, China
oulu9676@gmail.com; ORCID: 0000-0002-8441-781X

Shaolin Liao*
[1]*School of Electronics and Information Technology*
Sun Yat-sen University (SYSU)
Guangzhou, Guangdong, China
[2]*Electrical and Computer Engineering*
Illinois Institute of Technology
Chicago, IL, USA
liaoshlin@sysu.edu.cn; ORCID: 0000-0002-4432-3448

Baiquan Liu
School of Electronics and Information Technology
Sun Yat-sen University (SYSU)
Guangzhou, Guangdong, China
liubq33@mail.sysu.edu.cn

Xianbo Li
School of Electronics and Information Technology
Sun Yat-sen University (SYSU)
Guangzhou, Guangdong, China
lixianbo3@mail.sysu.edu.cn

Qingqing Ke
School of Microelectronics Science and Technology
Sun Yat-sen University (SYSU)
Zhuhai, Guangdong, China
keqingq@mail.sysu.edu.cn

Zhengji Xu
School of Microelectronics Science and Technology
Sun Yat-sen University (SYSU)
Zhuhai, Guangdong, China
xuzhj27@mail.sysu.edu.cn; ORCID: 0000-0002-0265-6228

Shuyan Zhu
School of Microelectronics Science and Technology
Sun Yat-sen University (SYSU)
Zhuhai, Guangdong, China
zhushy27@mail.sysu.edu.cn; ORCID: 0000-0003-1393-9271

Gengzhen Qi
School of Microelectronics Science and Technology
Sun Yat-sen University (SYSU)
Zhuhai, Guangdong, China
qigzh@mail.sysu.edu.cn; ORCID: 0000-0001-5035-8017

***Abstract*—As Multiple Inputs Multiple Outputs (MIMO) is becoming one of the enable techniques in modern wireless communication like 5G/6G and beyond, it is important to design efficient controls for the MIMO antenna arrays to realize critical functions such as high-throughput communication and beamforming. Efficient and rigorous Computational Electromagnetics (CEM) algorithms are key for such control design problem, especially for massive MIMO antenna arrays and beyond. Here we present such universal Fast Fourier Transform (FFT) based iterative CEM algorithm for efficient control design of massive MIMO antenna array and beyond, for example Reconfigurable Intelligent Surface and Large Intelligent Surface (RIS/LIS) MIMO. Our FFT-based iterative CEM algorithm is universal and works for both discrete MIMO and quasi-continuous RIS/LIS MIMO under various realistic amplitude and phase control constraints. It makes use of the translation invariant property of the dyadic function of the MIMO antenna arrays and compute the convolution operator in the spectral domain. Then it updates the control parameters iteratively under the control amplitude and control phase constraints, with the incident field and the target output field as inputs. Due to the use of FFT, the computational effort of the algorithm scales as $N \log N$ for $N = N_x \times N_y$ MIMO antennas, compared to N^3 of the direct solving method of the linear equation. Numerical simulation for 6G beamforming of both discrete MIMO and RIS/LIS MIMO under various control design constraints has been carried out to show the efficiency of the algorithm.**

***Index Terms*—Computational Electromagnetics (CEM), massive MIMO, Reconfigurable Intelligent Surface (RIS), Large Intelligent Surface (LIS), 5G, millimeter wave/THz 6G.**

*Shaolin Liao is the corresponding author and contributes equally as the first author.

Shaolin Liao is partially supported by start-up grant of SYSU's "100 Top Talents" Program under its "Academic Leaders" Category. Lu Ou is partially supported by the National Natural Science Foundation of China under Grant No.62002112, China Postdoctoral Science Foundation No. 2020M672488, Science and Technology Projects of Changsha City (kq2004027).

I. Introduction

Millimeter Wave (mmW: 30 GHz -300 GHz) and Terahertz (THz: 300 GHz -3 THz) boasts of a broad spectrum and has been widely considered for one of the next-generation 6G wireless communication techniques to resolve the ever increasing demand on data capacity and speed. Due to its smaller wavelength, mmW/THz 6G wireless communication allows for easy deployment of massive antenna arrays for Multiple Input Multiple Output (MIMO) wireless communication [1], [2], for example, Reconfigurable Intelligent Surface [3]–[8] and Large Intelligent Surface [9]–[11] (RIS/LIS) MIMO and even holographic MIMO [12], to realize many important functions such as beamforming [13], massive MIMO (mMIMO) wireless communication [14] and even Compressed Sensing (CS [15]–[19]) that makes use of the spatial diversity for higher data rate.

Thus MIMO control design becomes an important task to achieve the optimal performance of mmW/THz 6G wireless communication: to design the optimal control parameters for the MIMO antenna arrays, with the incident wave and the target output fields as the inputs. However, as the unknown control parameters scale as the MIMO antenna array size N, the direct solving method for the linear equation system requires the inverse of a $N \times N$ matrix, which means a computation effort of N^3. Such cubic scaling of the computation effort is unbearable due to the ever-increasing MIMO antenna array size N: from the discrete MIMO, to massive MIMO and quasi-continuous sub-wavelength RIS/LIS MIMO. Another issue that arises with the MIMO antenna arrays is the realistic constraints on control amplitude and phase of the MIMO antenna arrays, for which usually analytical optimized solution is not possible and numerical algorithm is required. All of the above call for efficient and scalable Computational Electromagnetics (CEM) design algorithm.

In this paper, we present such efficient CEM control design algorithm based on the Fast Fourier Transform (FFT) to accelerate the optimal control design of the MIMO antenna arrays. The FFT makes full use of the translation invariant property of the Green's function and solve the convolution equation in the spectral domain to realize an $N \times \log N$ computational time, as compared to the N^3 required by the direct solving method.

II. MIMO Design: Theoretical Formulation

Fig. 1a) shows the problem formulation for the MIMO design: the rectangular MIMO array consists of $N = N_x \times N_y$ antennas that has length periods of L_x, L_y in $\hat{x}, \hat{y}$ direction. The unknown parameters are the distributed surface current value $\mathbf{J}(\mathbf{x},\mathbf{y}) = \{\mathbf{J_x}(\mathbf{x},\mathbf{y}), \mathbf{J_y}(\mathbf{x},\mathbf{y}), \mathbf{J_z}(\mathbf{x},\mathbf{y})\}$ of the $N = N_x \times N_y$ antennas. Assuming linear excitation of the MIMO antenna unit cell, the distributed surface current value $J(x, y)$ is proportional to only the excitation field for all (x, y) location. So the unknown parameter $\mathbf{J}(x, y)$ can be reduced to the surface current of some anchor point of the MIMO antenna unit cell, for example, the geometric center. Let's denote such unknown surface current values at the anchor points of the MIMO array in the vector format as $\overline{\mathbf{J}}_N$. Similarly, the incident field upon the MIMO antenna array is denoted as vector $\overline{\mathbf{E}}^i_N$ and the target output field is denoted as vector $\overline{\mathbf{E}}^o_N$.

Without loss of generality, we assume that the controlled surface current values at the anchor points of the controlled MIMO array is given by

$$\overline{\mathbf{J}}_N = \overline{\boldsymbol{C}}_N \cdot \overline{\mathbf{E}}^i_N, \tag{1}$$

where $\overline{\boldsymbol{C}}^i_N$ is the unknown complex control parameter vector that remains to be solved.

The output field $\overline{E}^o_N$ can be calculated from the surface current $\overline{I}_N$ as follows

$$\overline{\mathbf{E}}^o_N = \overline{\overline{\mathbf{L}}} \circledast \overline{\mathbf{J}}_N, \tag{2}$$

where $\overline{\overline{\mathbf{L}}}$ is the dyadic function and $\circledast$ denotes the spatial convolution. Thus, the surface current values at the anchor points of the MIMO antenna array $\overline{\mathbf{J}}_N$ can be solved as follows,

$$\overline{\mathbf{J}}_N = \overline{\overline{\mathbf{L}}}^{-1} \circledast \overline{\mathbf{E}}^o_N, \tag{3}$$

where $\overline{\overline{\mathbf{L}}}^{-1}$ is the inverse dyadic function of $\overline{\overline{\mathbf{L}}}$ that satisfies the following property

$$\overline{\overline{\mathbf{L}}}^{-1} \circledast \overline{\overline{\mathbf{L}}} = \overline{\overline{\mathbf{I}}}, \tag{4}$$

where $\overline{\overline{\mathbf{I}}}$ is the unit matrix.

Substituting Eq. (3) into Eq. (1), the linear equation of the collocation method is obtained

$$\overline{\mathbf{J}}_N = \overline{\overline{\mathbf{L}}}^{-1} \circledast \overline{\mathbf{E}}^o_N = \overline{\boldsymbol{C}}_N \cdot \overline{\mathbf{E}}^i_N, \tag{5}$$

which is the mathematical formulation of the MIMO control design problem.

A. Discrete MIMO Antenna Arrays

For discrete MIMO antenna arrays consisting of unit cell of finite size, the dyadic function $\overline{\overline{\mathbf{L}}}$ is actually the radiation pattern of each individual antenna. For example, the dyadic function in the far field for plane wave incidence upon a square metallic patch antenna in the far field under the Physical Optics (PO) approximation is given as follows [20],

$$\overline{\mathbf{L}}_{\theta x} \propto \sin\phi \cos\theta sinc\left(X\right) sinc\left(Y\right); \tag{6}$$

$$\overline{\mathbf{L}}_{\phi x} \propto \cos\phi \cos\theta sinc\left(X\right) sinc\left(Y\right), \tag{7}$$

where the far field is given for x-polarized incident field in the spherical coordinates (θ, ϕ). Similar expression can be obtained for y-polarized incident field.

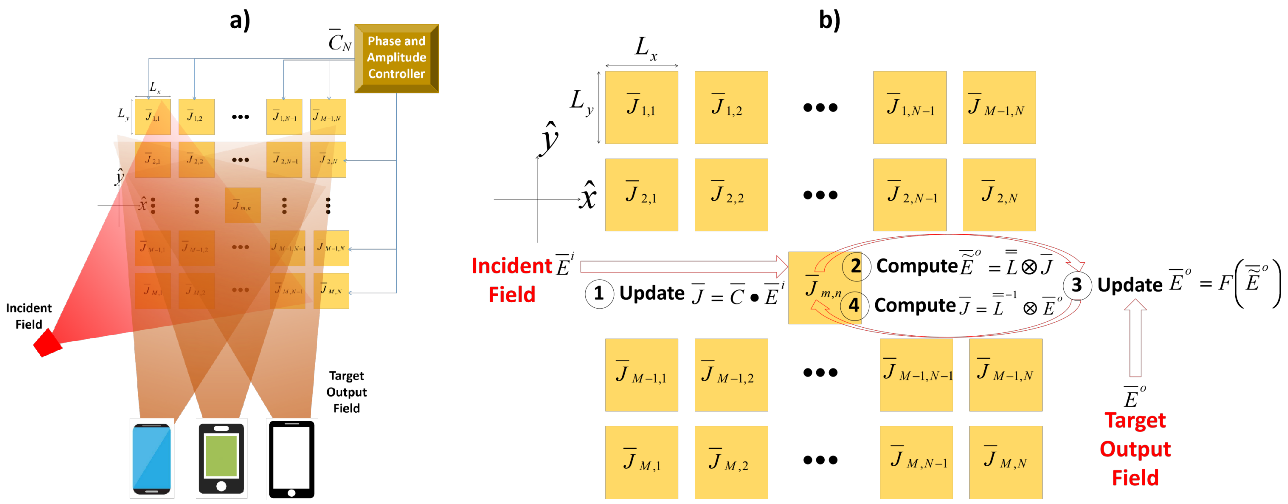

Fig. 1. MIMO control design problem formulation of an $N = N_x \times N_y$ MIMO antenna array with a unit cell area of $A = L_x \times L_y$: a) control design for MIMO beamforming; b) the FFT-based iterative CEM algorithm.

B. Quasi-continuous RIS/LIS MIMO

For continuous MIMO antenna arrays of infinitesimal small unit cell, the dyadic function $\overline{\overline{\mathbf{L}}}$ reduces to the dyadic Green's function $\overline{\overline{\mathbf{G}}}^e$ given as follows [21],

$$\overline{\overline{\mathbf{G}}}^e = \left(1 + \frac{1}{k^2}\nabla\nabla\cdot\right) g\left(\mathbf{r}, \mathbf{r}'\right) \overline{\overline{I}}, \tag{8}$$

where $g\left(\mathbf{r}, \mathbf{r}'\right)$ is the scalar Green's function at the observation point $\mathbf{r}$ due to the source point $\mathbf{r}'$.

III. MIMO Control Design: the FFT-based CEM Algorithm

One issue to solve the surface current values at the anchor points of the MIMO antenna array $\overline{\mathbf{J}}_N$ of Eq. (5) is that, it requires the inverse of the dyadic function $\overline{\overline{\mathbf{L}}}$, which means N^3 computation effort. However, due to the spatial translation invariant of the convolution, FFT and Inverse FFT (IFFT) can be used to accelerate the computation as follow [21], [22]

$$\overline{\mathbf{J}}_N = \text{IFFT}\left\{ \overline{\overline{\boldsymbol{\mathcal{L}}}}^{-1} \overline{\boldsymbol{\mathcal{E}}}_N^o \right\}, \tag{9}$$

where $\overline{\overline{\boldsymbol{\mathcal{L}}}}$ and $\overline{\boldsymbol{\mathcal{C}}}_N$ are the Fourier transformed spectra of the dyadic function $\overline{\overline{\mathbf{L}}}$, and the control parameter at the anchor points of the MIMO antenna array respectively.

A. Exact Complex Control

For MIMO antenna array that can be controlled exactly in both amplitude and phase, the control parameter $\overline{\boldsymbol{\mathcal{C}}}_N$ of Eq. (5) can be readily obtained as follows

$$\overline{\boldsymbol{\mathcal{C}}}_N = \frac{\text{IFFT}\left\{ \overline{\overline{\boldsymbol{\mathcal{L}}}}^{-1} \overline{\boldsymbol{\mathcal{E}}}_N^o \right\}}{\overline{\mathbf{E}}_N^i}. \tag{10}$$

B. Digital Control

Another issue remains to be solved is that, due to realistic constraints of technique and cost, MIMO amplitude and phase control might be limited. For example, only digital amplitude and digital phase are available. Under such situation, an analytical solution of Eq. (5) is not possible and calls for iterative algorithm that updates the control amplitude and phase at each iteration [22]–[25].

Here we study such iterative CEM algorithm based on FFT for efficient control design of MIMO antenna arrays under various amplitude and phase constraints. As shown in Fig. 1b), the FFT-based iterative CEM algorithm follows the procedure given below,

1) Compute the surface current $\overline{\mathbf{J}}_N$ with the target output field $\overline{\mathbf{E}}_N^o$ according to Eq. (9);
2) Update the control parameter $\overline{\mathbf{C}}_N$ according to Eq. (1) with the surface current $\overline{\mathbf{J}}_N$ and the incident field $\overline{\mathbf{E}}_N^i$;
3) Apply digital amplitude and phase constraints on the control parameter $\left[\overline{\mathbf{C}}_N\right]$;
4) Update the constrained surface current $\left[\overline{\mathbf{J}}_N\right]$ with the constrained control parameter $\left[\overline{\mathbf{C}}_N\right]$;
5) Compute output field $\overline{\mathbf{E}}_N^o$ according to Eq. (2) with the constrained surface current $\left[\overline{\mathbf{J}}_N\right]$;
6) Update the target output field $\overline{\mathbf{E}}_N^o$ by keeping its phase while replacing its amplitude pattern by the designed amplitude pattern;
7) Go to Step 1) and repeat till the preset convergence criterion is satisfied.

C. Phase-only Control

When only phase control is available, the iterative CEM algorithm is similar to that for digital control in Section III-B, except applying uniform amplitude constraint.

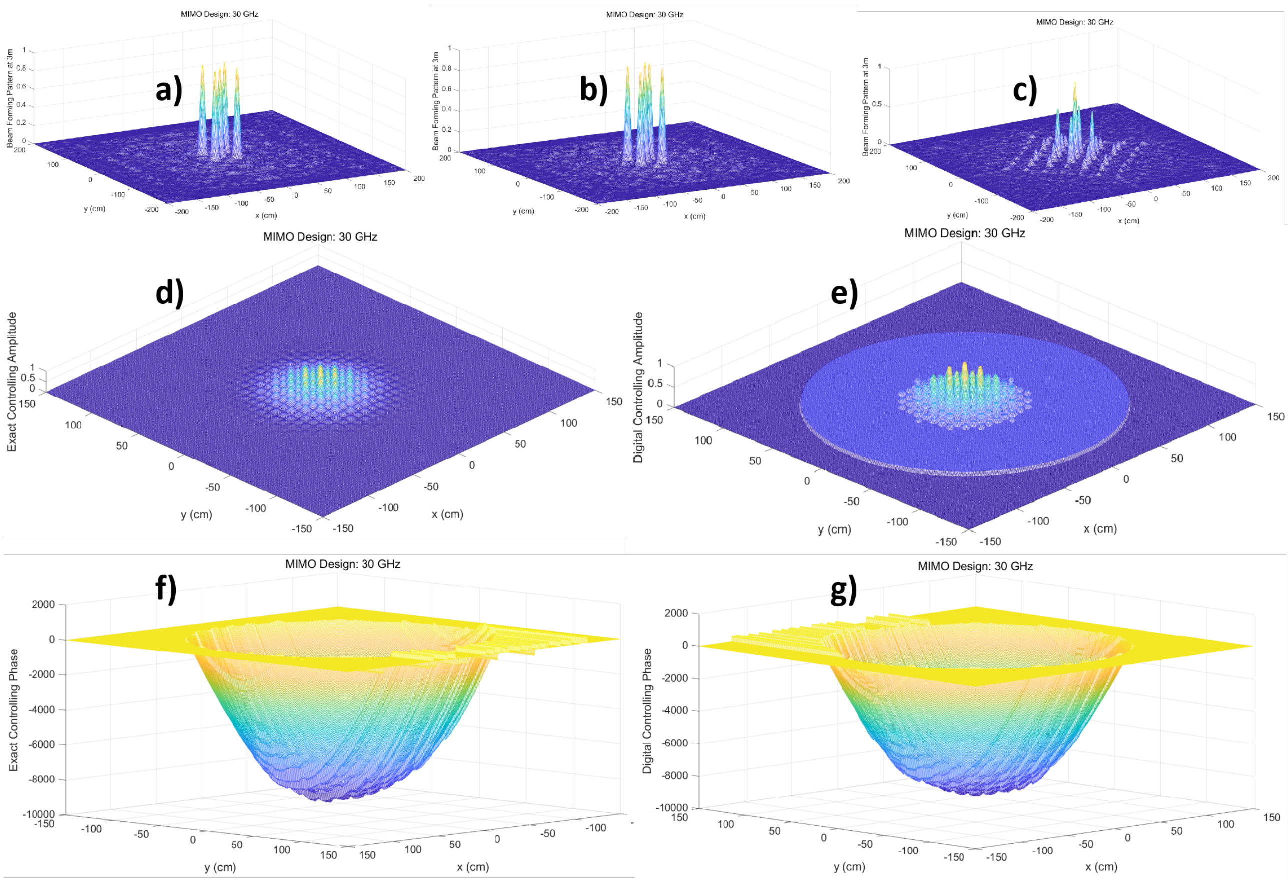

Fig. 2. Sparse beamforming MIMO control design: a) Beam pattern at 3m for exact complex control; b) Beam pattern at 3m for digital control; c) Beam pattern at 3m for digital phase-only control; d) control amplitude of the exact complex control; e) control amplitude of the digital control; f) control phase of the exact complex control; g) digital control phase of the digital control and the phase-only control.

IV. MIMO Control Design: Examples

The quasi-continuous sub-wavelength RIS/LIS MIMO array has attracted increasing attention, especially for the upcoming millimeter-wave/THz 6G wireless communication. Here two RIS/LIS MIMO control design examples are given to show how Eq. (10) can be used to efficiently solve the unknown control parameter $\overline{\boldsymbol{C}}_N$ of the MIMO antenna array: 1) sparse beamforming; 2) OAM beamforming. In all simulation, a digital amplitude of 0.1 incremental scale or resolution and digital phase of 45° incremental scale or resolution have been used. Also, square RIS/LIS MIMO antennas with negligible gaps are used, with a unit cell area of $0.1\lambda \times 0.1\lambda$ inside which the surface current can be approximately considered as uniform. Finally, the incident field is a Gaussian beam.

A. *Sparse beamforming*

In the dynamic wireless communication environment, mobile users are moving around. Thus steering communication energy to mobile users can avoid wasting energy and increase the Signal to Noise Ratio (SNR) of the wireless communication, which means higher data rate according to the Shannon's theorem. For such reason, it is desirable to design optimal sparse beamforming RIS/LIS MIMO control under its amplitude and phase constraints. Here we design such sparse beamforming pattern with 5 smartphone communication locations with equal communication energy. Finally, the Gaussian width of the incident field is 25λ, while that of the target sparse output field is 5λ.

1) Exact Complex Control: Fig. 2a) shows the obtained sparse MIMO beamforming pattern at a distance of 3m for exact complex control and Fig. 2d), Fig. 2f) show the corresponding control amplitude and phase respectively. It can be seen that, with exact complex control without any amplitude and phase constraint, the designed beamforming pattern behaves well and all five beam spots are well identified with small side lobes are other locations.

2) Digital Control: Similarly, Fig. 2b) shows the obtained sparse MIMO beamforming pattern at a distance of 3m for digital control and Fig. 2e), Fig. 2g) show the corresponding control amplitude and phase respectively. It can be seen that, with digital amplitude and digital phase control, the designed beamforming pattern contains bigger side lobes at other locations.

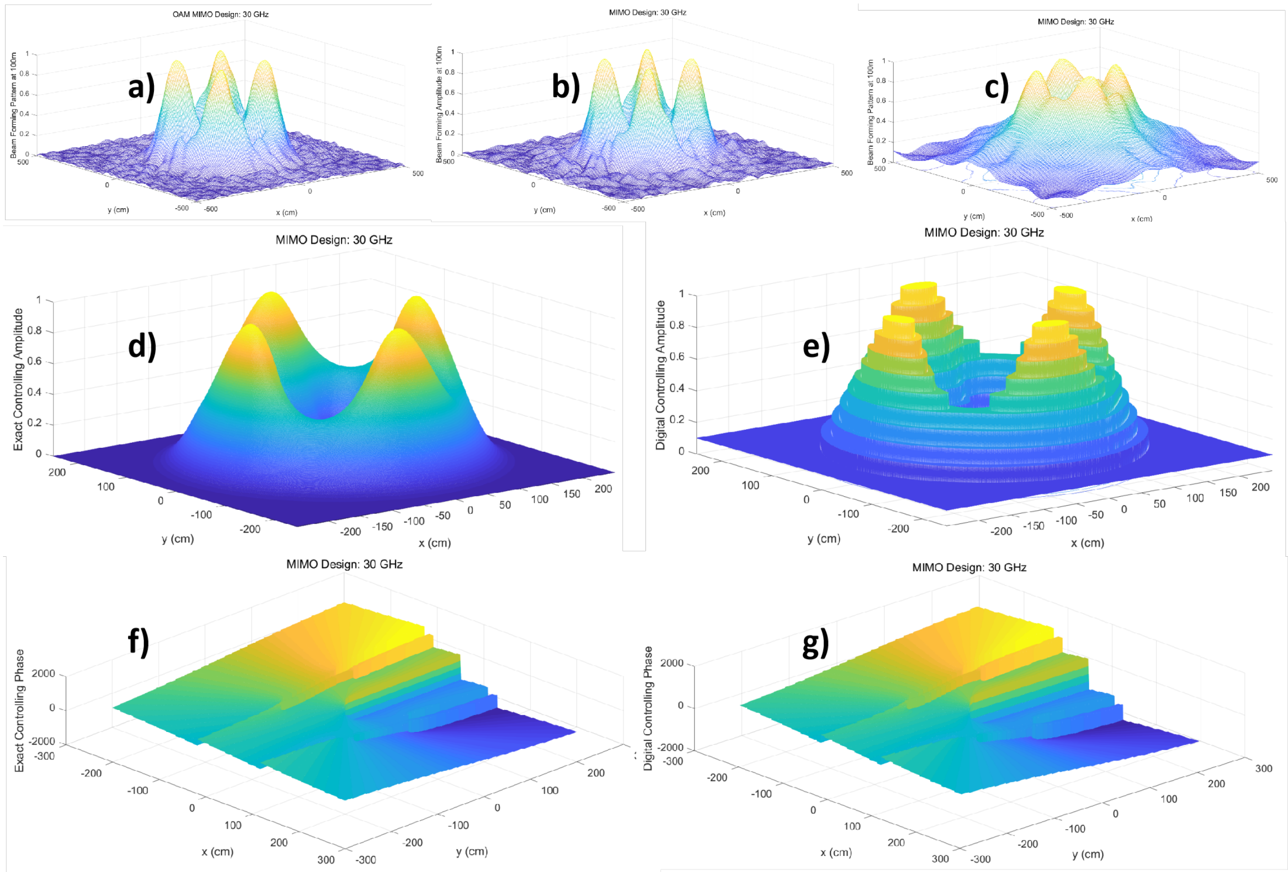

Fig. 3. OAM beamforming MIMO control design: a) Beam pattern at 3m for exact complex control; b) Beam pattern at 3m for digital control; c) Beam pattern at 3m for digital phase-only control; d) control amplitude of the exact complex control; e) control amplitude of the digital control; f) control phase of the exact complex control; g) digital control phase of the digital control and the phase-only control.

3) Phase-only Control: At last, Fig. 2c) shows the obtained sparse MIMO beamforming pattern at a distance of 3m for digital phase-only control, from which it can be seen that more and bigger side lobes appear at a much larger area. However, it still roughly forms 5 communication spot locations.

B. OAM beamforming

OAM is a special type of MIMO communication that has its unique property such as coherent spatial phase that can be used to increase the SNR and thus the wireless communication data rate. Here we design such OAM beamforming pattern with 4 smartphone communication locations with equal communication energy. Finally, the Gaussian width of the incident field is 100λ, while that of the target OAM output field is 50λ.

1) Exact Complex Control: Fig. 3a) shows the obtained OAM MIMO beamforming pattern at a distance of 100m for exact complex control and Fig. 3d), Fig. 3f) show the corresponding control amplitude and phase respectively. It can be seen that four OAM communication spot locations clearly show up, as expected.

2) Digital Control: Similarly, Fig. 3b) shows the obtained OAM MIMO beamforming pattern at a distance of 100m for digital control and Fig. 3e), Fig. 3g) show the corresponding control amplitude and phase respectively. It can be seen that satisfied OAM beamforming pattern still can be obtained, though with bigger side lobes spreading into a larger area.

3) Phase-only Control: At last, Fig. 3c) shows the obtained OAM MIMO beamforming pattern at a distance of 100m for digital phase-only control, from which it can be seen that the four OAM spot location overlaps with each other and bigger side lobes spread into a even larger area.

V. Conclusion

An FFT-based iterative CEM algorithm has been developed for universal control of massive MIMO and beyond. The algorithm is universal and works for both discrete MIMO antenna arrays and quasi-continuous RIS/LIS MIMO antenna arrays. Numerical simulation has been performed for both sparse beamforming and OAM beamforming, under three control constraints: exact complex control, digital control and phase-only control. The results show that the FFT-based iterative CEM algorithm is efficient in design of arbitrary control amplitude and phase for massive MIMO and beyond, with a computation effort scales as $N \log N$ for an $N = N_x \times N_y$ MIMO antenna array.

REFERENCES

[1] B. Li, Z. Zhang, Z. Hu, and Y. Chen, "Joint Array Diagnosis and Channel Estimation for RIS-Aided mmWave MIMO System," IEEE Access, vol. 8, pp. 193992–194006, 2020, doi: 10.1109/ACCESS.2020.3032775.

[2] S. Sun, A. P. Petropulu, and H. V. Poor, "MIMO Radar for Advanced Driver-Assistance Systems and Autonomous Driving: Advantages and Challenges," IEEE Signal Processing Magazine, vol. 37, no. 4, pp. 98–117, Jul. 2020, doi: 10.1109/MSP.2020.2978507.

[3] H. Yang, X. Cao, F. Yang, J. Gao, S. Xu, M. Li, X. Chen, Y. Zhao, Y. Zheng and S. Li, "A programmable metasurface with dynamic polarization, scattering and focusing control," *Scientific Reports,* vol. 6, no. 1, p. 35692, 2016.

[4] W. Tang *et al.*,"MIMO Transmission Through Reconfigurable Intelligent Surface: System Design, Analysis, and Implementation,"IEEE J. on Selected Areas in Communications, vol. 38, no. 11, pp. 2683-2699, Nov. 2020, DOI.org/10.1109/JSAC.2020.3007055.

[5] X. Yang, C.-K. Wen, and S. Jin, "MIMO Detection for Reconfigurable Intelligent Surface-Assisted Millimeter Wave Systems," IEEE Journal on Selected Areas in Communications, vol. 38, no. 8, pp. 1777–1792, Aug. 2020, doi: 10.1109/JSAC.2020.3000822.

[6] W. Tang *et al.*, "MIMO Transmission Through Reconfigurable Intelligent Surface: System Design, Analysis, and Implementation," IEEE Journal on Selected Areas in Communications, vol. 38, no. 11, pp. 2683–2699, Nov. 2020, doi: 10.1109/JSAC.2020.3007055.

[7] E. Basar, "Reconfigurable Intelligent Surface-Based Index Modulation: A New Beyond MIMO Paradigm for 6G," IEEE Transactions on Communications, vol. 68, no. 5, pp. 3187–3196, May 2020, doi: 10.1109/TCOMM.2020.2971486.

[8] M. Nemati, J. Park, and J. Choi, "RIS-Assisted Coverage Enhancement in Millimeter-Wave Cellular Networks," IEEE Access, vol. 8, pp. 188171–188185, 2020, doi: 10.1109/ACCESS.2020.3031392.

[9] D. Dardari, "Communicating With Large Intelligent Surfaces: Fundamental Limits and Models," IEEE Journal on Selected Areas in Communications, vol. 38, no. 11, pp. 2526–2537, Nov. 2020, doi: 10.1109/JSAC.2020.3007036.

[10] B. Li, Z. Zhang, Z. Hu, and Y. Chen, "Joint Array Diagnosis and Channel Estimation for RIS-Aided mmWave MIMO System," IEEE Access, vol. 8, pp. 193992–194006, 2020, doi: 10.1109/ACCESS.2020.3032775.

[11] P. Wang, J. Fang, L. Dai, and H. Li, "Joint Transceiver and Large Intelligent Surface Design for Massive MIMO mmWave Systems," IEEE Transactions on Wireless Communications, vol. 20, no. 2, pp. 1052–1064, Feb. 2021, doi: 10.1109/TWC.2020.3030570.

[12] C. Huang *et al.*, "Holographic MIMO Surfaces for 6G Wireless Networks: Opportunities, Challenges, and Trends," IEEE Wireless Communications, vol. 27, no. 5, pp. 118–125, Oct. 2020, doi: 10.1109/MWC.001.1900534.

[13] E. Bjornson, L. Van der Perre, S. Buzzi and E. G. Larsson, "Massive MIMO in sub-6 GHz and mmW: physical, practical, and use-case differences," *IEEE Wirel. Commun.* 26, 100-108 (2019).

[14] R. Chataut and R. Akl, "Massive MIMO Systems for 5G and beyond Networks - Overview, Recent Trends, Challenges, and Future Research Direction," Sensors (Basel), vol. 20, no. 10, May 2020, doi: 10.3390/s20102753.

[15] L. Ou and S. Liao, Z. Qin and H. Yin, "Millimeter Wave Wireless Hadamard Image Transmission for MIMO Enabled 5G and Beyond," in *IEEE Wireless Communications*, 2020, doi: 10.1109/MWC.001.2000081.

[16] N. Gopalsami *et al.* , "Passive millimeter-wave imaging with compressive sensing," *Optical Engineering*, 51(9), 091614, 2012.

[17] S.D. Babacan, M. Luessi, L. Spinoulas, A.K. Katsaggelos, N. Gopalsami, T. Elmer, R. Ahern, S. Liao and A, Raptis, "Compressive passive millimeter-wave imaging," *18th IEEE International Conference on Image Processing 2011*, Brussels, Belgium, 2011. DOI.org/10.1109/ICIP.2011.6116227

[18] N. Gopalsami, S. Liao, T. W. Elmer, A. Heifetz, A. C. Raptis, "Compressive sampling in active and passive millimeter-wave imaging," *2011 International Conference on Infrared, Millimeter, and Terahertz Waves*, Houston, TX, USA, Oct. 2-7, 2011. DOI.org/10.1109/irmmw-THz.2011.6105205

[19] N. Gopalsami, S. Liao, T. W. Elmer, E. R. Koehl, A. Heifetz and A. C. Raptis; *Compressive passive millimeter wave imager,* 2015-1-27, US Patent, US20130257646A1.

[20] C. A. Balanis, *Advanced Engineering Electromagnetics,* John Wiley & Sons, 1989.

[21] S. Liao, *Millimeter-wave Techniques: Theory, Algorithms and Methods,* engrXiv, DOI.org/10.31224/osf.io/y8p9t

[22] S. Liao, R. J. Vernon, "A Fast Algorithm for Computation of Electromagnetic Wave Propagation in Half-Space," *IEEE Transactions on Antennas and Propagation*, 2009, 57(7): 2068-2075. DOI.org/10.1109/TAP.2009.2021890

[23] L. Ou and S. Liao, "A Ping-Pong Algorithm for Computational Electromagnetics of 2D Antennas/Metasurfaces," *2020 IEEE Asia-Pacific Microwave Conference (APMC)*, Hong Kong, Dec. 8-11, 2020. DOI.org/10.1109/APMC47863.2020.9331423

[24] S. Liao, L. Ou, "Iterative Physical Optics (IPO) for Fast and Accurate Simulation of Reflector Antennas," *2020 IEEE Asia-Pacific Microwave Conference (APMC)*, Hong Kong, Dec. 8-11, 2020. DOI.org/10.1109/APMC47863.2020.9331679

[25] S. Liao, N. Gopalsami, A. Venugopal, A. Heifetz and A. C. Raptis, "An efficient iterative algorithm for computation of scattering from dielectric objects," *Optics Express*, 2011, 19(4): 3304-3315. DOI.org/10.1364/OE.19.003304